J Appl Electrochem (2007) 37:877–886
DOI 10.1007/s10800-007-9324-2

ORIGINAL PAPER

Effect of leakage currents on the primary current distribution in bipolar electrochemical reactors

E.R.Henquín · J.M.Bisang

Received: 2 January 2007 / Accepted: 8 March 2007 / Published online: 7 April 2007

Abstract The primary current distribution in a bipolar electrochemical reactor with outside inlet and outlet electrolyte manifolds was investigated by numerical solution of the Laplace equation and by experimental measurement in simulated cells made from conductive paper and segmented electrodes. The geometric parameters determining the distribution were the interelectrode gap, electrode length, transverse section and length of the electrolyte manifold. The effect of the number of electrodes in the bipolar stack was also analysed. Values obtained numerically have been compared with those obtained experimentally and a good agreement is observed between them. These results are useful for estimating the performance of the bipolar stack.

Keywords Bipolar electrodes · Current distribution · Electrochemical reactors · Laplace equation · Leakage current

List of symbols

a	Geometric parameter of the manifold (m)
A	Transverse section of the electrolyte manifold (m^2)
b	Geometric parameter of the manifold (m)
$\overline{d}_r$	Mean relative deviation (%)
e	Interelectrode gap (m)
G	Length of the electrolyte manifold (m)
j	Current density (A m^{-2})
j_{mean}	Mean current density (A m^{-2})
I	Total current (A)
I^*	Leakage current (A)
I_B	Total current at the bipolar electrode (A)
L	Electrode length (m)
n	Number of bipolar electrodes
N	Number of experimental values in Eq. 7
R	By-pass resistance (Ω)
U	Applied voltage to the reactor (V)
U_A	Potential at the terminal anode (V)
U_C	Potential at the terminal cathode (V)
W	Electrode width (m)
x	Axial coordinate (m)
y	Axial coordinate (m)
z	Normalized y axial coordinate = y/L

Greek characters

φ	Potential in the solution phase (V)
λ	Dimensionless number given by Eq. 6
ρ	Electrolyte resistivity (Ω m)
σ	Standard deviation

Subscripts

A	Terminal anode
B_k	kth bipolar electrode
C	Terminal cathode

1 Introduction

In recent years there has been an increasing interest in the use of bipolar reactors for electrochemical processes. Generally the electrolyte is fed to the individual bipolar cells via inlet and outlet manifolds; and leakage currents, also called parasitic, shunt or by-pass currents, flowing

E. R. Henquín · J. M. Bisang (✉)
Programa de Electroquímica Aplicada e Ingeniería Electroquímica (PRELINE), Facultad de Ingeniería Química (UNL), Santiago del Estero 2829, S3000AOM Santa Fe, Argentina
e-mail: jbisang@fiqus.unl.edu.ar

through the connecting manifolds and pipes diminish the current efficiency of the bipolar cell stack. Several authors [1–12] reported procedures for calculating leakage currents and current efficiency but little attention was paid to the effect of leakage currents on the potential and current distribution in terminal and bipolar electrodes. Thus, Divisek et al. [13] computed the potential profile in electrolysers by numerical solution of the Laplace equation using the finite difference method. The potential profile was related to the potential-dependent thermodynamic stabilities of the respective metals in order to determine corrosion zones in the bipolar stack. Bonvin [14] solved the Laplace equation for a bipolar electrochemical reactor and reported experimental results of current distributions. Rousar and Thonstad [15] informed about the calculation of by-pass currents and current distribution in molten salt bipolar cells with open channels to allow the circulation of the electrolyte. Recently, in [16] a simplified mathematical model to calculate the current distribution in bipolar electrochemical reactors was developed and comparisons between calculated and experimental primary current distributions were reported. This model satisfactorily predicted the current distribution at the terminal electrodes for the highest by-pass resistances.

The aim of the present work is to analyse the effect of leakage currents on the primary current distribution at the electrodes in an undivided bipolar stack by numerical solution of the Laplace equation and to corroborate the results experimentally.

2 Theoretical considerations

A bipolar electrochemical stack consists of one anode A, n bipolar electrodes B_n and one cathode C. Each inside reactor of the stack is composed of the anodic side of a bipolar electrode, the cathodic side of the next bipolar electrode and between them the electrolyte. The outermost reactors of the stack include the terminal anode A or the terminal cathode C. Each reactor has manifolds for the inlet and outlet of the electrolyte which generate leakage currents. Figure 1 schematically shows the configuration of an electrochemical reactor with n bipolar electrodes.

In the following mathematical treatment some simplifying assumptions are made:

(i) The metal phase of the electrodes is isopotential.
(ii) The overpotentials at the interfaces are neglected, thus primary current distributions will be obtained.
(iii) The current distribution in the direction of the electrode width is neglected.
(iv) For symmetry only one half of the reactor is considered.

Thus, in order to obtain the potential distribution, it is necessary to solve the Laplace equation in the solution phase including the electrolyte manifolds:

$$\frac{\partial^2\phi}{\partial x^2}+\frac{\partial^2\phi}{\partial y^2}=0 \tag{1}$$

subject to the following boundary conditions: at the terminal anode,

$$\phi = U_{\mathrm{A}} \tag{2}$$

at the terminal cathode,

$$\phi = U_{\mathrm{C}} \tag{3}$$

and at the insulating walls

$$\left.\frac{\partial\phi}{\partial x}\right|_{\text{insulating walls}}=0 \tag{4}$$

The current density at any point at the electrode surface is given by:

$$\left.\frac{\partial\phi}{\partial x}\right|_{\text{ith electrode surface}}=-\rho j_{\mathrm{i}} \text{ with i = A, } \mathrm{B_k} \text{ or C} \tag{5}$$

Equation 1 was numerically solved by the finite difference method with an equidistant grid in order to obtain the potential distribution and the local current density at each electrode surface was evaluated according to Eq. 5 from the numerical determination of the local potential gradient perpendicular to the surface.

2.1 Effect of the electrolyte manifold dimensions

Figure 2 shows the potential distribution for a typical case and Fig. 3 reports the effect of the electrolyte manifold length on the current distribution for an electrochemical stack with one bipolar electrode, for symmetry only one half of the reactor is plotted. As expected, the current distribution at the terminal electrodes shows a maximum at the end point and a minimum in the central region. Thus, the more pronounced variation in the current density occurs at the ends of the electrodes, which can be explained taking into account that the region near the inlet or outlet of the electrolyte can offer a larger contribution to the leakage current than the central region of the electrodes. Likewise, the current distribution becomes more pronounced when the electrolyte manifold length decreases because the leakage current increases. The number six curves, with the shorter length, correspond to a reactor with an inside electrolyte manifold. The current distribution at the bipolar electrode is more uniform than

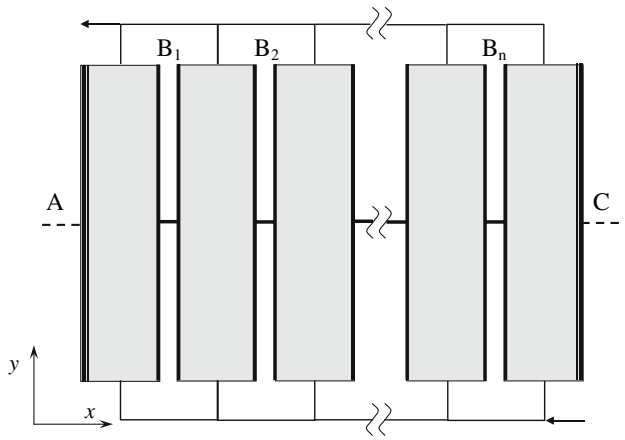

Fig. 1 Schematic representation of a bipolar electrochemical stack. ▬ : terminal electrodes, — : bipolar electrodes, ▭ : electrolyte, — : electrolyte manifold, – – : electric contact to the terminal electrodes

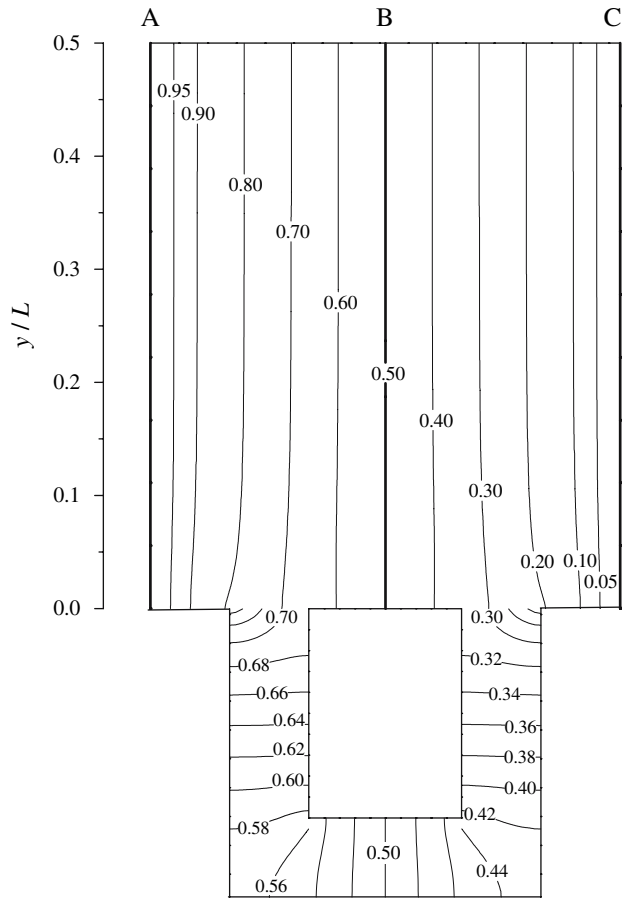

Fig. 2 Potential distribution for an electrochemical stack with one bipolar electrode. G = 78.5 mm, L = 100 mm, e = 20 mm, A/eW = 0.35. The potentials are referred to the anode potential

at the terminal electrode and it shows a minimum of current density at points near the electrode end, but the minimum shows a displacement to the electrode end when the electrolyte manifold length decreases, which is a

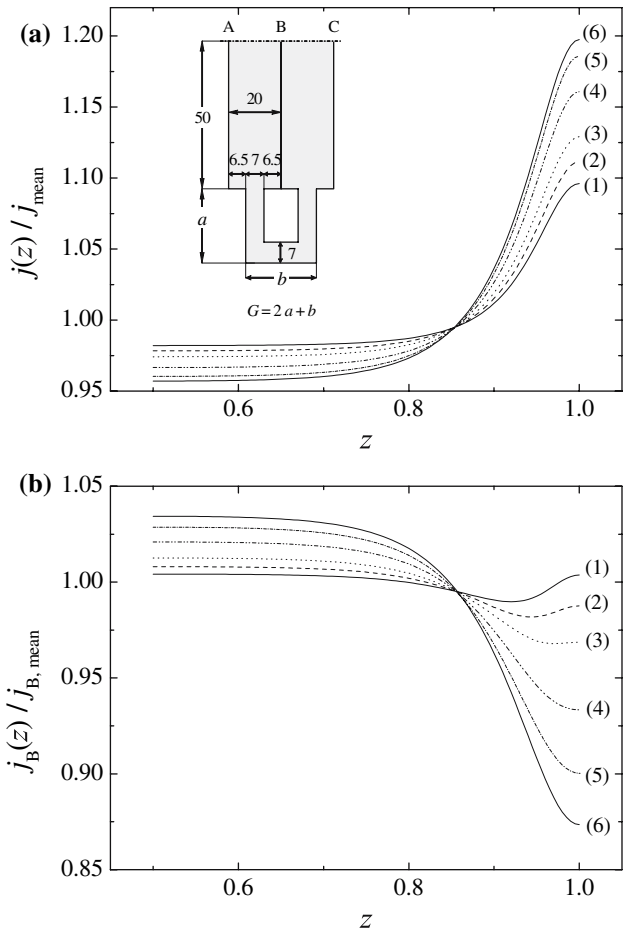

Fig. 3 Current distributions for different values of the electrolyte manifold length. One bipolar electrode. (**a**) terminal electrodes, (**b**) bipolar electrode. (1): G = 128.5 mm, (2): G = 98.5 mm, (3): G = 78.5 mm, (4): G = 58.5 mm, (5): G = 48.5 mm, (6): G = 43.5 mm. L = 100 mm, e = 20 mm, A/eW = 0.35. Inset: arrangement of the electrochemical reactor with inlet manifold. Dimensions in mm

consequence of the fact that the supply and discharge nozzles for the electrolyte represent only a fraction of the cross sectional area of the interelectrode gap.

Figure 4 shows current distributions for different ratios between the transverse section of the electrolyte manifold and the cross sectional area of the interelectrode gap. It can be confirmed that an increase in the transverse section of the electrolyte manifold has the same effect as a decrease in the electrolyte manifold length.

2.2 Effect of the interelectrode gap and electrode length

Figure 5 shows the current distribution as a function of the electrode length for a 20 mm interelectrode gap. The current distribution becomes more uneven when L increases because the regions far from the electrolyte inlet

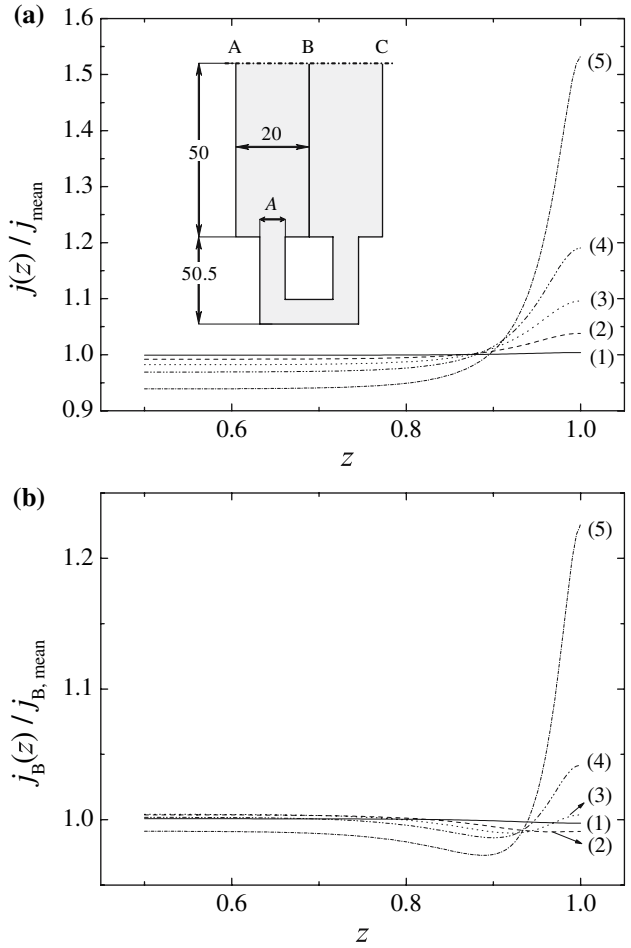

Fig. 4 Current distributions for different values of the ratio between the transverse section of the electrolyte manifold and the cross sectional area of the interelectrode gap. One bipolar electrode. (**a**) terminal electrodes, (**b**) bipolar electrode. (1): A/eW = 5%, (2): A/eW = 20%, (3): A/eW = 35%, (4): A/eW = 50%, (5): A/eW = 75%. L = 100 mm, e = 20 mm. Inset: arrangement of the electrochemical reactor with inlet manifold. Dimensions in mm

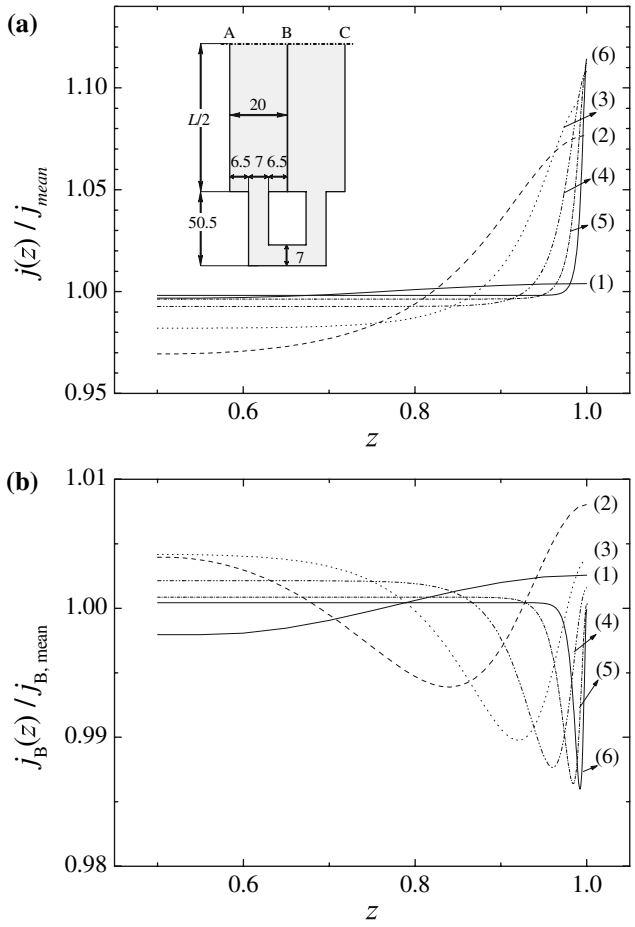

Fig. 5 Current distributions as a function of the electrode length L for a given configuration of the inlet and outlet manifold. One bipolar electrode. Part (**a**): terminal electrodes, Part (**b**): bipolar electrode. (1): L = 10 mm, (2): L = 50 mm, (3): L = 100 mm, (4): L = 250 mm, (5): L = 500 mm, (6): L = 1,000 mm. e = 20 mm. A / eW = 0.35. Inset: arrangement of the electrochemical reactor with inlet manifold. Dimensions in mm

do not contribute to the leakage current [16]. However, in the case of high electrode length, typical in industrial reactors, the terminal electrodes show prominent current distributions only at small regions near the inlet and outlet manifolds, approximately 5% of the electrode length, and the remaining electrode surface works with a current density near the mean value. Figure 5 part (b) reports that the current distribution at the bipolar electrode shows a minimum close to the inlet and outlet manifolds. However, comparing parts (a) and (b) in Fig. 5, it can be observed that the current distribution at the bipolar electrodes is less pronounced that at the terminal electrodes due to the damping effect of the electrolyte solution. Figure 6 shows the current distribution as a function of the interelectrode gap for a given electrolyte path in the manifold. From Figs. 5 and 6, it can be observed that an increase in the interelectrode gap has the same effect on the current distribution as a decrease in the electrode length. Thus, both parameters can be lumped in a dimensionless number, λ, which characterizes the reactor geometry defined as [16]:

$$\lambda = \frac{2L^2}{e^2} \tag{6}$$

An increase in λ produces uneven current distributions. However, the effect of the interelectrode gap on the current distribution is more pronounced than the effect of electrode length.

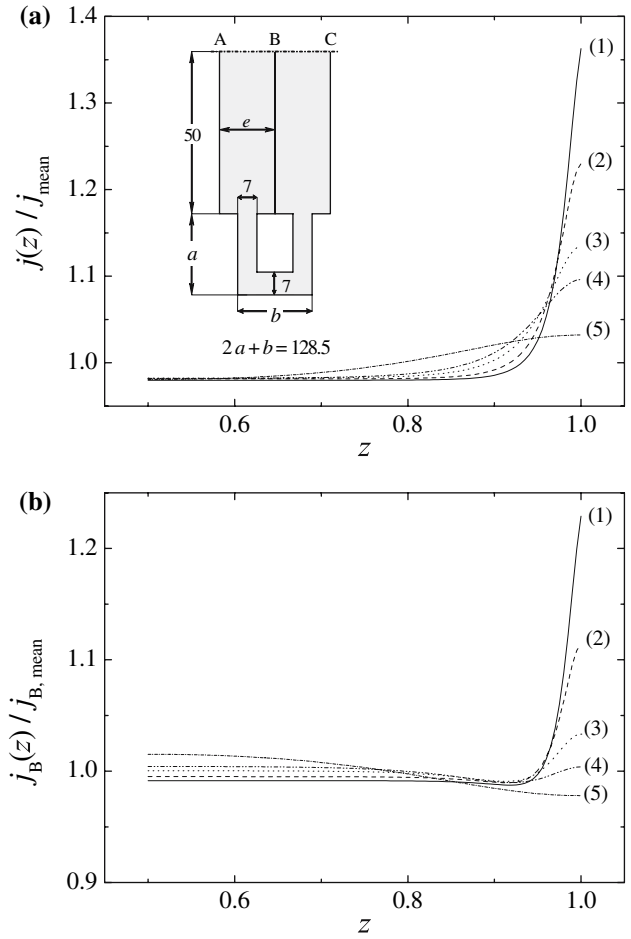

Fig. 6 Current distributions as a function of the interelectrode gap e for a given configuration of the inlet and outlet manifold. One bipolar electrode. Part (**a**): terminal electrodes, Part (**b**): bipolar electrode. (1): e = 10 mm, (2): e = 12 mm, (3): e = 16 mm, (4): e = 20 mm, (5): e = 50 mm. L = 100 mm. Inset: arrangement of the electrochemical reactor with inlet manifold. Dimensions in mm

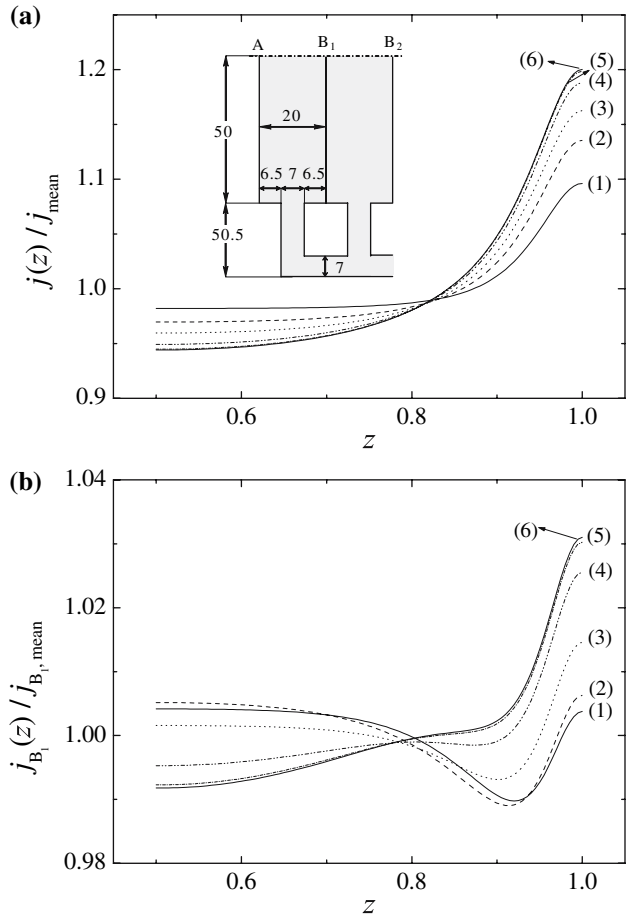

Fig. 7 Effect of the number of electrodes in the bipolar electrochemical stack on the current distributions. (**a**) terminal electrode, (**b**) first bipolar electrode. (1): stack with one bipolar electrode, (2): stack with two bipolar electrodes, (3): stack with three bipolar electrodes, (4): stack with five bipolar electrodes, (5): stack with eight bipolar electrodes, (6): stack with ten bipolar electrodes. L = 100 mm, e = 20 mm, A/eW = 0.35. Inset: arrangement of the electrochemical reactor with inlet manifold. Dimensions in mm

Comparing Figs. 3 and 4 with Figs. 5 and 6 it is observed that an increase in λ has the same effect on the current distribution as a decrease in G/A.

2.3 Current distributions as a function of the number of bipolar electrodes

Figure 7 shows the current distribution in electrochemical stacks with a different number of bipolar electrodes, part (a) corresponds to the terminal electrodes and part (b) to the bipolar electrode closest to the terminal electrodes. It can be seen that the current distributions at the terminal electrodes becomes more pronounced when the number of bipolar electrodes is increased. However, in a stack with a large number of bipolar electrodes, more than eight, the current distribution is not modified. The same behaviour is detected in the current distribution at the bipolar electrode which is nearest to the terminal electrode. However, the current distribution at this electrode is less significant.

Figure 8 shows the current distributions at the different electrodes in an electrochemical stack with ten bipolar electrodes. As inset, the standard deviation relative to the mean current density for each electrode is given. Figure 8 reveals that only the terminal electrodes show a significant current distribution and the bipolar electrodes present similar values but lower than the terminal electrodes.

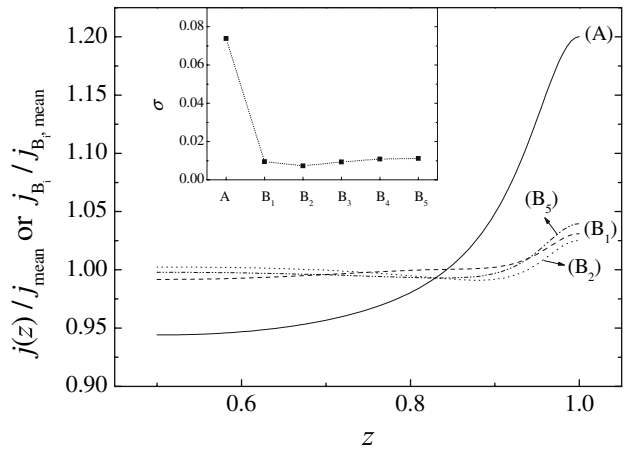

Fig. 8 Current distributions for an electrochemical stack with ten bipolar electrodes. (A): Terminal electrodes, (B_1): first bipolar electrode, (B_2): second bipolar electrode, (B_5): fifth bipolar electrode. L = 100 mm, e = 20 mm, A/eW = 0.35. Other dimensions according to the inset in Fig. 7. Inset: Standard deviation of the current distributions relative to the mean current density for each electrode

3 Comparison with experimental results of primary current distribution

3.1 Experimental

Figure 9 depicts the experimental arrangement. The electrolyte at each reactor of the bipolar electrochemical stack was simulated by a sheet of conductive paper (Pasco Scientific, PK 9025) mounted on a non-conducting board and the electrodes were formed by fifteen copper segments, 6.1 × 10^{-3} m wide, at opposite sides of the conductive paper. The segments were insulated from one another by an approximately 5 × 10^{-4} m thick Teflon slide and were connected to the conductive paper by colloidal silver paint (Pasco Scientific, PK-9031B) in order to minimize the contact resistance. The current distribution at each electrode was determined by measuring the ohmic drops in calibrated resistors, approximately 30 Ω resistance, which were intercalated between each segment and the current feeder for the terminal electrodes and between the corresponding anodic and cathodic segments for the bipolar electrodes. The effect of the calibrated resistors on the current distribution can be neglected due to the small value of their resistance in comparison to that of the conductive paper. The data acquisition was performed using a computer controlled, home made analogue multiplexer. The interelectrode gap was 0.021 m and the conductive paper and segments were trimmed to give a length of 0.1 m. The thickness of the conductive paper was 1.3 × 10^{-4} m and the resistivity was 3.48 Ω m. The

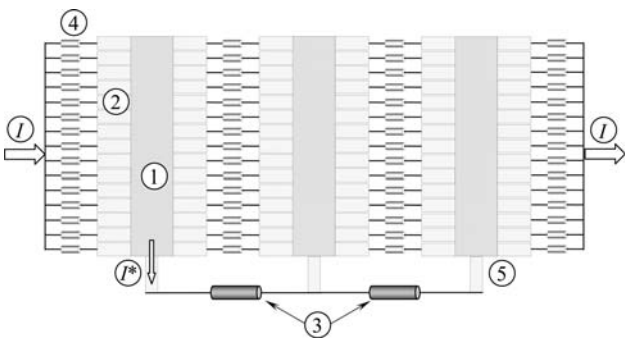

Fig. 9 Schematic view of the experimental arrangement. (1) conductive paper, (2) segmented electrodes, (3) by-pass resistors, (4) calibrated resistors, (5) electric contact

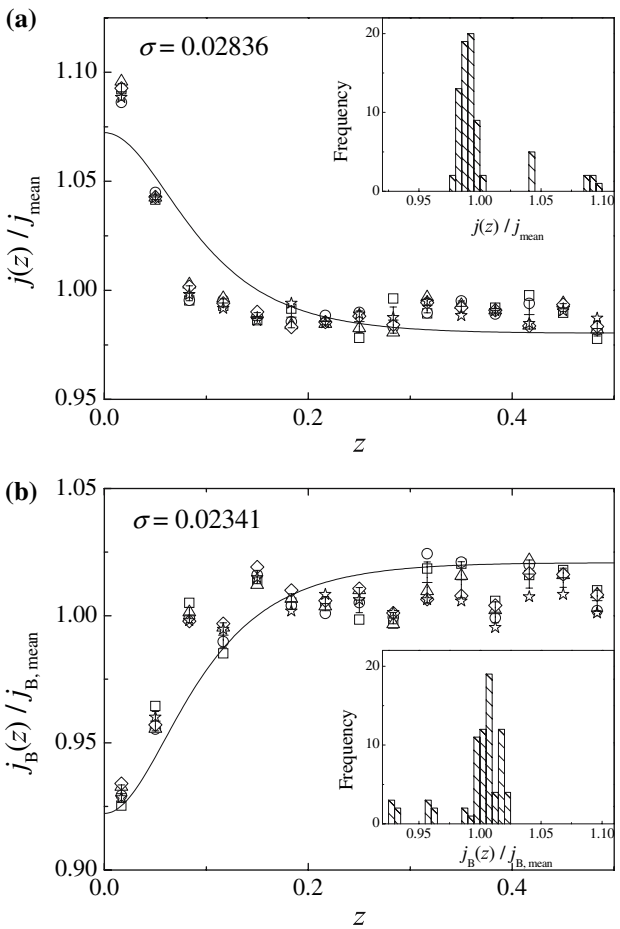

Fig. 10 Primary current distributions for an electrochemical stack with one bipolar electrode. (**a**) terminal electrodes, (**b**) bipolar electrode. (□): I = 5.01 mA, (○): I = 3.99 mA, (△) : 3.00 mA , (◇): I = 1.98 mA, (☆): I = 0.98 mA. (+): mean value, (I): standard deviation for different total currents. R = 99,608 Ω. Full line: numerical solution of the Laplace equation. Inset: histogram of j/j_{mean}

inlet manifold was also simulated by by-pass resistors. For symmetry reasons only one half of the reactor was simulated. A dc power supply was used to apply a constant current to the feeders. The electric connection was made at the mid point of the current feeder of each terminal electrode. For a given value of the by-pass resistance several experiments were carried out for different total currents in order to test the reproducibility of the results.

3.2 Results and discussion

Figure 10 shows typical results of current distribution at the terminal and bipolar electrodes for different values of total current when the experimental arrangement presents one bipolar electrode. Figure 11 reports the case of two bipolar electrodes. The full lines correspond to the solution of the Laplace equation by the finite difference method. A histogram of the experimental current densities is included as an inset in each figure in order to show the deviations of the current densities from the mean value. The standard deviation of the experimental current distributions related to the mean current density is also given. As expected for a given value of by-pass resistance the distributions are independent of the total current and a close agreement between the experimental points and the theoretical calculations is observed. The small differences between them can be attributed to the contact resistance between the segment and the conductive paper, in spite of the special attention paid to these joints. The experimental measurements also represent mean values of current density at each segment.

Table 1 and 2 summarize the results obtained with one and two bipolar electrodes respectively. To quantify the agreement between the experimental current distributions and those obtained from the solution of the Laplace equation, in columns 3 and 4, the mean relative deviation $\overline{d}_r$ is given, which is defined as:

$$\overline{d}_r = \frac{1}{N}\sum_{i=1}^{N}\frac{\left|j_{exp}(z_i) - j_{th}(z_i)\right|}{j_{th}(z_i)}100 \qquad (7)$$

Lower values of $\overline{d}_r$ imply close agreement between the two distributions. From Tables 1 and 2 it is observed that $\overline{d}_r$ is near 1%. Likewise, column 8 in Tables 1 and 2 shows the error between the theoretical and experimental values of the cell voltage and the leakage current and a minor error is also observed.

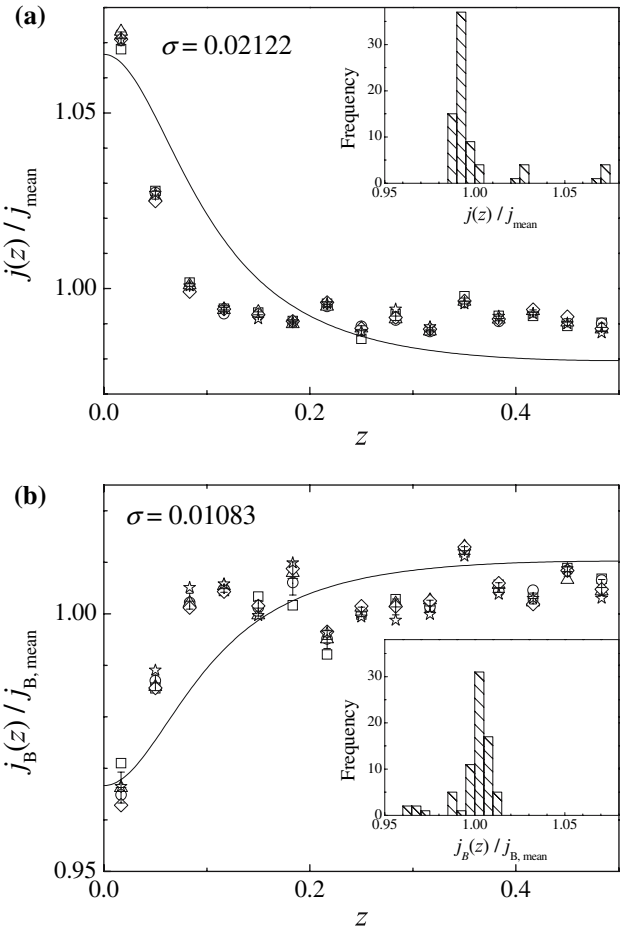

Fig. 11 Primary current distributions for an electrochemical stack with two bipolar electrodes. (**a**) terminal electrodes. (**b**) bipolar electrode. (□): I = 3.54 mA, (○): I = 3.03 mA, (△) : 2.52 mA, (◇): I = 2.00 mA, (☆):I = 100 mA. (+): mean value, (I): standard deviation for different total currents. R = 150,600 Ω. Full line: numerical solution of the Laplace equation. Inset: histogram of j/j_{mean}

4 Conclusions

(i) A close agreement for the primary current distributions, cell voltage and leakage current was obtained for bipolar electrochemical reactors with outside inlet and outlet electrolyte manifolds by using two methods: numerical solution of the Laplace equation and experimental measurements in simulated cells.

(ii) Leakage currents produce uneven current distributions in the reactor. The current distributions are more pronounced for small by-pass resistance and higher values of a parameter λ, which characterizes the geometry of the reactor.

Table 1 Summary of experimental results for one bipolar electrode

R (Ω)	I (mA)	$\overline{d}_r$ (%)			Theoretical values	Experimental values	Error (%)
		Terminals	Bipolar				
99,608	0.98	1.03	1.36	U (V)	10.91	11.10	1.79
				I^* (mA)	0.0388	0.0380	1.92
	1.98	1.05	1.16	U (V)	22.07	22.15	0.37
				I^* (mA)	0.0785	0.0773	1.50
	3.00	1.06	1.07	U (V)	33.40	33.10	0.90
				I^* (mA)	0.1190	0.1171	1.55
	3.99	1.03	1.08	U (V)	44.50	43.90	1.35
				I^* (mA)	0.1584	0.1553	1.91
	5.01	1.22	1.05	U (V)	55.93	54.85	1.93
				I^* (mA)	0.1989	0.1955	1.74
150,552	0.98	0.69	1.29	U (V)	10.95	11.15	1.79
				I^* (mA)	0.0285	0.0278	2.43
	1.98	0.81	1.37	U (V)	22.23	22.30	0.32
				I^* (mA)	0.0578	0.0576	0.44
	3.00	0.82	1.27	U (V)	33.61	33.35	0.76
				I^* (mA)	0.0875	0.0875	0.00
	3.99	0.73	1.25	U (V)	44.81	44.40	0.90
				I^* (mA)	0.1165	0.1166	0.02
	5.02	0.81	1.12	U (V)	56.30	55.35	1.69
				I^* (mA)	0.1465	0.1458	0.49
322,206	0.96	0.65	1.04	U (V)	10.81	11.20	3.63
				I^* (mA)	0.0151	0.0136	9.96
	1.97	0.48	0.94	U (V)	22.25	22.35	0.45
				I^* (mA)	0.0310	0.0301	3.11
	2.98	0.49	0.86	U (V)	33.68	33.55	0.39
				I^* (mA)	0.0470	0.0464	1.28
	4.00	0.84	1.04	U (V)	45.50	44.55	2.09
				I^* (mA)	0.0629	0.0629	0.00
	5.02	0.54	0.91	U (V)	56.65	55.75	1.59
				I^* (mA)	0.0792	0.0796	0.56
447,435	0.97	0.45	0.60	U (V)	10.98	11.20	2.02
				I^* (mA)	0.0111	0.0098	12.20
	1.97	0.44	0.62	U (V)	22.26	22.45	0.86
				I^* (mA)	0.0226	0.0209	7.34
	2.98	0.37	0.48	U (V)	33.76	33.65	0.33
				I^* (mA)	0.0343	0.0331	3.33
	3.98	0.32	0.55	U (V)	45.02	44.90	0.27
				I^* (mA)	0.0457	0.0442	3.34
	4.99	0.35	0.38	U (V)	56.50	55.85	1.15
				I^* (mA)	0.0576	0.0567	1.59

Table 2 Summary of experimental results for two bipolar electrodes

R (Ω)	I (mA)	$\overline{d}_r$ (%)			Theoretical values	Experimental values	Error (%)
		Terminals	Bipolars				
99,608	0.97	1.75	1.46	U (V)	15.75	16.00	1.59
				I^* (mA)	0.0449	0.0420	6.46
	1.99	1.73	1.20	U (V)	32.13	31.85	0.88
				I^* (mA)	0.0916	0.0865	5.57
	2.49	1.61	1.26	U (V)	40.31	39.85	1.15
				I^* (mA)	0.1150	0.1083	5.83
	3.01	1.55	1.20	U (V)	48.76	48.00	1.55
				I^* (mA)	0.1391	0.1317	5.32
	3.51	1.67	1.37	U (V)	56.82	56.05	1.35
				I^* (mA)	0.1620	0.1537	5.12
150,600	1.00	1.14	1.26	U (V)	16.32	16.05	1.66
				I^* (mA)	0.0323	0.0304	5.88
	2.00	1.17	1.06	U (V)	32.85	32.15	2.12
				I^* (mA)	0.0650	0.0618	4.92
	2.52	1.14	1.08	U (V)	41.17	40.15	2.49
				I^* (mA)	0.0815	0.0777	4.66
	3.03	1.18	1.02	U (V)	49.40	48.25	2.33
				I^* (mA)	0.0978	0.0933	4.60
	3.54	1.11	1.08	U (V)	57.80	56.35	2.51
				I^* (mA)	0.1147	0.1091	4.88
316,826	1.00	0.62	1.13	U (V)	16.48	16.40	0.45
				I^* (mA)	0.0164	0.0153	6.71
	2.02	0.59	0.92	U (V)	33.29	32.90	1.16
				I^* (mA)	0.0332	0.0313	5.72
	2.52	0.51	0.84	U (V)	41.60	41.05	1.33
				I^* (mA)	0.0415	0.0392	5.54
	3.03	0.55	0.84	U (V)	49.95	49.30	1.30
				I^* (mA)	0.0498	0.0471	5.42
	3.54	0.47	0.95	U (V)	58.40	57.45	1.63
				I^* (mA)	0.0582	0.0551	5.33
447,435	0.99	0.64	1.07	U (V)	16.37	16.55	1.10
				I^* (mA)	0.0117	0.0100	14.53
	2.01	0.46	0.82	U (V)	33.25	33.10	0.45
				I^* (mA)	0.0238	0.0218	8.40
	2.52	0.50	0.83	U (V)	41.68	41.15	1.26
				I^* (mA)	0.0299	0.0276	7.69
	3.02	0.51	0.82	U (V)	50.06	49.35	1.42
				I^* (mA)	0.0359	0.0333	7.24
	3.53	0.46	0.88	U (V)	58.54	57.65	1.51
				I^* (mA)	0.0419	0.0389	7.16

(iii) In a bipolar electrochemical stack current distribution is important at the terminal electrodes but it is less significant at the bipolar electrodes.

Acknowledgements This work was supported by the Agencia Nacional de Promoción Científica y Tecnológica (ANPCyT), Consejo Nacional de Investigaciones Científicas y Técnicas (CONICET) and Universidad Nacional del Litoral (UNL) of Argentina.

References

1. Rousar I (1969) J Electrochem Soc 116:676
2. Rousar I, Cezner V (1974) J Electrochem Soc 121:648
3. Katz M (1978) J Electrochem Soc 125:515
4. Burnett JC, Danly DE (1979) AIChE Symp Ser 75:8
5. Khun AT, Booth JS (1980) J Appl Electrochem 10:233
6. Thiele W, Schleiff M, Matschiner H (1981) Electrochim Acta 26:1005
7. Kaminski EA, Savinell RF (1983) J Electrochem Soc 130:1103
8. White RE, Walton CW, Burney HS, Beaver RN (1986) J Electrochem Soc 133:485
9. Seiger HN (1986) J Electrochem Soc 133:2002
10. Comninellis Ch, Plattner E, Bolomey P (1991) J Appl Electrochem 21:415
11. Bonvin G, Comninellis Ch (1994) J Appl Electrochem 24:469
12. Rangarajan SK, Yegnanarayanan V (1997) Electrochim Acta 42:153
13. Divisek J, Jung R, Britz D (1990) J Appl Electrochem 20:186
14. Bonvin G (1992) Swiss Federal Institute of Technology, Lausanne, thesis 1029
15. Rousar I, Thonstad J (1994) J Appl Electrochem 24:1124
16. Henquín ER, Bisang JM (2005) J Appl Electrochem 35:1183